ANTIOXIDANTS & REDOX SIGNALING
Volume 15, Number 9, 2011

DOI: 10.1089/ars.2010.3857

ORIGINAL RESEARCH COMMUNICATION

Defective Leptin–AMP-Dependent Kinase Pathway Induces Nitric Oxide Release and Contributes to Mitochondrial Dysfunction and Obesity in *ob/ob* Mice

Paola V. Finocchietto,[1,2] Silvia Holod,[1,3] Fernando Barreyro,[1] Jorge G. Peralta,[1,2] Yael Alippe,[1,2] Andrés Giovambattista,[4,5] María C. Carreras,[1,3,5,*] and Juan J. Poderoso[1,2,5,*]

Abstract

Aims: Obesity arises on defective neuroendocrine pathways that increase energy intake and reduce mitochondrial metabolism. In the metabolic syndrome, mitochondrial dysfunction accomplishes defects in fatty acid oxidation and reciprocal increase in triglyceride content with insulin resistance and hyperglycemia. Mitochondrial inhibition is attributed to reduced biogenesis, excessive fission, and low adipokine-AMP-activated protein kinase (AMPK) level, but lateness of the respiratory chain contributes to perturbations. Considering that nitric oxide (NO) binds cytochrome oxidase and inhibits respiration, we explored NO as a direct effector of mitochondrial dysfunction in the leptin-deficient *ob/ob* mice. ***Results:*** A remarkable three- to fourfold increase in neuronal nitric oxide synthase (nNOS) expression and activity was detected by western blot, citrulline assay, electronic and confocal microscopy, flow cytometry, and NO electrode sensor in mitochondria from *ob/ob* mice. High NO reduced oxygen uptake in *ob/ob* mitochondria by inhibition of complex IV and nitration of complex I. Low metabolic status restricted β-oxidation in obese mitochondria and displaced acetyl-CoA to fat synthesis; instead, small interference RNA nNOS caused a phenotype change with fat reduction in *ob/ob* adipocytes. ***Innovation:*** We evidenced that leptin increases mitochondrial respiration and fat utilization by potentially inhibiting NO release. Accordingly, leptin administration to *ob/ob* mice prevented nNOS overexpression and mitochondrial dysfunction *in vivo* and rescued leptin-dependent effects by matrix NO reduction, whereas leptin–Ob-Rb disruption increased the formation of mitochondrial NO in control adipocytes. We demonstrated that in *ob/ob*, hypoleptinemia is associated with critically low mitochondrial p-AMPK and that, oppositely to p-Akt2, p-AMPK is a negative modulator of nNOS. ***Conclusion:*** Thereby, defective leptin–AMPK pathway links mitochondrial NO to obesity with complex I syndrome and dysfunctional mitochondria. *Antioxid. Redox Signal.* 15, 2395–2406.

Introduction

OBESITY RESULTS FROM AN IMBALANCE between energy intake and expenditure, and this imbalance has brought about a pandemic responsible for increased morbidity and mortality rates in western society (19).

Insulin resistance is an important feature of obesity and the metabolic syndrome (MS). In these conditions, increased fatty acids are mobilized from adipose tissue and ectopically accumulated in liver, skeletal muscle, and β cells, resulting in dysregulated glucose metabolism, lipid induced insulin resistance, inflammation, increased reactive oxygen species production, and decrease in mitochondrial biogenesis. This phenotypic expression is linked to inactivation of leptin–AMP-activated protein kinase (AMPK) and p-AMPK-PCG1α pathways (43).

Innovation

Obesity is a severe pandemia associated with leptin deficiency or resistance. It is shown here that leptin-deficient obesity is contributed by high mitochondrial nitric oxide synthase at low AMP-activated protein kinase level with nitric oxide-induced adipose mitochondrial dysfunction.

[1]Laboratory of Oxygen Metabolism, University Hospital, [2]Department of Internal Medicine, School of Medicine, and [3]Department of Clinical Biochemistry, School of Pharmacy and Biochemistry, University of Buenos Aires, Buenos Aires, Argentina.
[4]IMBICE University of La Plata, Buenos Aires, Argentina.
[5]Consejo Nacional de Investigaciones Científicas y Técnicas, La Plata, Argentina.
*These two authors equally contributed to this work.

Leptin regulates the balance of energy by stimulating neuropeptide Y neurons to promote satiety; in addition, leptin plays a peripheral role in increasing the metabolic rate and energy consumption (11, 35). Leptin resistance is a prominent feature in obese subjects with hypometabolism and also characterizes MS; hyperleptinemia itself contributes to the development of leptin resistance (26). A well-known model of MS is the *ob/ob* mouse that carry a premature stop codon in the *Lep* gene, which forms truncated mRNA and results in inactive leptin; pure leptin deficiency is rare in humans (34). Mitochondria in *ob/ob* mice have an abnormally high matrix volume and fewer cristae than normal mouse mitochondria. These characteristics are accompanied by reduced oxygen uptake and adenosine triphosphate (ATP) production (2), uncoupled oxidative phosphorylation, low mitochondrial complex activity, and increased nitration-nitrosylation of mitochondrial proteins (16, 17).

Nitric oxide (NO) is a typical modulator of oxidative metabolism by reversibly inhibiting the Cu^{2+}-Fe center of cytochrome oxidase (1, 4, 6) (Supplementary Fig. S1A; Supplementary Data are available online at www.liebertonline.com/ars). We have previously shown that NO inhibition in mitochondria increases the mitochondrial production of superoxide anion and hydrogen peroxide (41) to yield peroxynitrite ($ONOO^-$), a nitrating-nitrosylating compound resulting from the direct reaction between NO and superoxide anion (42, 44) (Supplementary Fig. S1). Additionally, we recently reported that neuronal nitric oxide synthase (nNOS) translocates into mitochondria (5, 8–10, 18) and that the resultant mitochondrial nitric oxide synthase (mtNOS) is allosterically and positively regulated in skeletal muscle by the mitochondrial insulin/p-Akt2 pathway (14). Therefore, in the present study, we hypothesized that leptin deficiency and insulin resistance induces mitochondrial dysfunction through mitochondrial NO excess that contributes to the general mechanism of insufficient activation of the AMPK signaling pathways and to obesity.

Results

High NO yield in ob/ob mitochondria

Considering NO inhibitory effects on mitochondrial respiration (6, 41) and obese mitochondrial dysfunction as resulting from increased oxidative and nitrative damage (16), the first step toward understanding the mechanisms of hypoleptinemia was to assess NO level in the *ob/ob* mice. A remarkable increase in nNOS expression was detected here in *ob/ob* epididymal white adipose tissue (WAT) (Fig. 1A). Using quantitative real-time polymerase chain reaction (PCR), a fourfold increase in nNOS gene transcriptional activity was

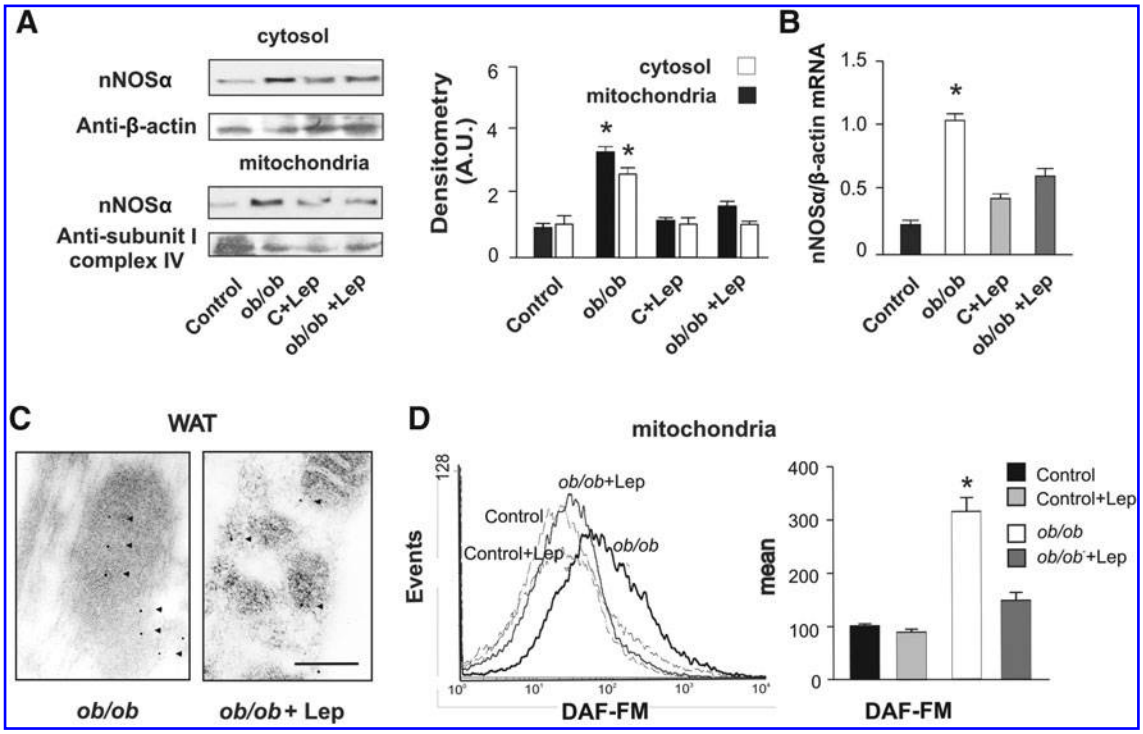

FIG. 1. Leptin deficiency induces high neuronal nitric oxide synthase (nNOS) and nitric oxide (NO) in *ob/ob* adipose tissue. (A) Differential nNOS expression in white adipose tissue (WAT) from control C57BL/6 and *ob/ob* mice before and after *in vivo* treatment with leptin; purified mitochondria were treated with 50 μg/ml proteinase K. Bars reflect densitometries in arbitrary units (A.U.; mean ± standard error of the mean [SEM], $n = 6$); $^*p < 0.05$ *versus* control by analysis of variance and Dunnett's test. **(B)** Comparative nNOS mRNA expression was quantified by quantitative real-time–polymerase chain reaction of adipocyte lysates; mean ± SEM, $n = 3$, $^*p < 0.05$ *versus* control. **(C)** *Left*: Immunoelectron microscopy of adipose tissue shows intramitochondrial gold particles linked to a monoclonal anti-nNOS ab (1:400) in adipose *ob/ob* tissue; *right*, immune staining show decrease of the signal in *ob/ob* treated with leptin. No signal was detected in absence of ab (not shown); bar = 400 nm. **(D)** Modulation of mitochondrial NO by leptin is represented by flow-cytometric histograms in isolated and purified *ob/ob* adipose organelles stained with 4-amino-5-methylamino-2′,7′-difluorofluorescin diacetate (DAF-FM); on the *right*, bars represent median peak fluorescence of the populations (mean ± SEM, $n = 5$); $^*p < 0.05$ *versus* control.

detected, and the resultant nNOS protein was proportionally distributed between the cytosol (+160%) and mitochondria (+270%), indicating active nNOS trafficking into the organelles (13) (Fig. 1B, C); inducible NO synthase or endothelial nitric oxide synthase (eNOS) was not detected. Administration of leptin to *ob/ob* mice *in vivo* for 4 days abrogated the nNOS overexpression in WAT (Fig. 1A, B). Increased nNOS trafficking in *ob/ob* mice was revealed by immune electron microscopy of WAT and also it was reduced after leptin administration (Fig. 1C). Translocated nNOS efficiently increased matrix NO yield in the adipose tissue. According to nNOS expression, flow cytometry analysis of isolated organelles stained with the NO indicator 4-amino-5-methylamino-2′,7′-difluorofluorescin diacetate (DAF-FM) confirmed higher steady-state NO concentrations in WAT of *ob/ob* respect to *wt* mice (+200%±24%, $p<0.0001$), a result similarly reverted by *in vivo* leptin administration (Fig. 1D).

To search for a link between fat content and mitochondrial NO, we explored adipocytes with confocal microscopy. Control C57BL/6 *wt* adipocytes exhibit discrete NO level in peripherically distributed mitochondria. Instead, *ob/ob* adipocytes had significant NO colocalization within marginal mitochondria and increased cell volume because of high fat accumulation (Fig. 2). We then challenged *ob/ob* adipocytes with nNOS small interference RNA (siRNA); transfection was ~40% efficient and exhibited no intrinsic activity in *ob/ob* adipocytes. nNOS expression was reduced by 60% with respect to the empty vector. The loss of mitochondrial NO by the silencing of nNOS resulted in a decrease in cell volume (~27%) and fat content and in a more homogeneous mitochondrial distribution (see Supplementary Figures).

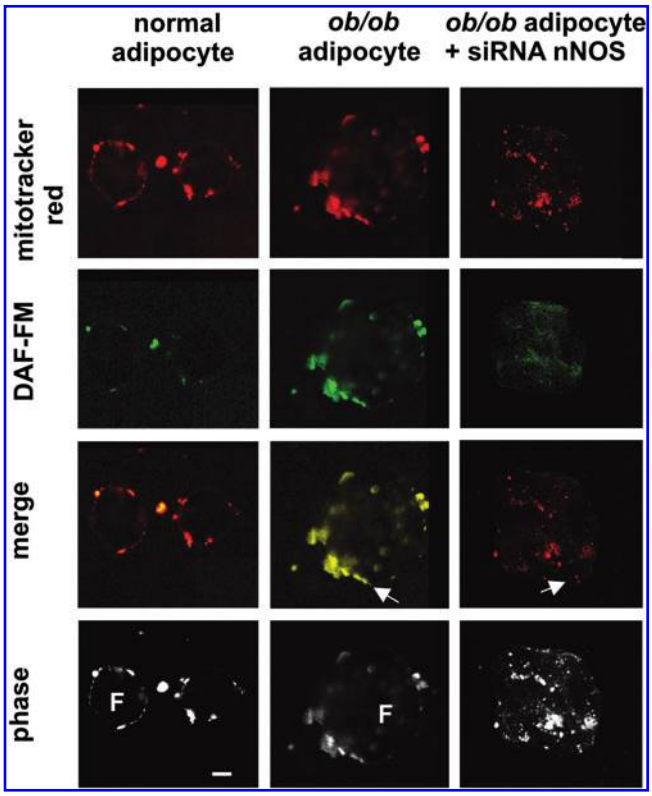

FIG. 2. Differential fat content correlates with mitochondrial NO steady-state concentration in the adipocyte phenotypes. Adipocytes were obtained from fat pads with collagenase. The images show confocal microscopic images of isolated *wt* C57BJ/6 and *ob/ob* adipocytes stained with Mitotracker and DAF-FM. In the *right lane*, the nNOS knockdown in *ob/ob* adipocytes is shown. *Ob/ob* cells were transfected with 10 μg nNOS small interference RNA (siRNA), and 24 h later, deficient adipocytes have lost NO and fat. Images are representative of 2–3 experiments. Phase is single channel *gray color* mode. *White arrows*, mitochondria; *white bar*, 30 μm; F, fat.

Increase of cytosol and, particularly, of mitochondrial NO yield in *ob/ob* with respect to control samples was as well detected by measuring nNOS activity (+2–3-fold in cytosol and +3–4-fold in mitochondria from adipose and liver tissues respectively; Table 1). NO release by isolated liver mitochondria was also significantly higher in *ob/ob* mice than in controls (+4-fold; Table 1).

In accord, high nNOS levels were also detected in non-adipose tissue from *ob/ob* mice (Supplementary Fig. S2A, B), but inducible NO synthase or eNOS was not found in mitochondria (not shown). Comparatively, skeletal muscle and liver mitochondria from *ob/ob* mice had less *ex vivo* NO than WAT but still significantly more than controls (values as mean±standard error of the mean [SEM]; WAT: +250%±22%; skeletal muscle: +131%±14%; and liver: +66%±9%; $n=7$; $p<0.0001$) (Fig. 3A); DAF fluorescence was almost abolished in the *ob/ob* mitochondria after incubation with the NOS inhibitor L-N^G-methyl-L-arginine (L-NMMA), and fluorescence was not detected in control organelles with substantially less mtNOS activity, as detected by electron microscopy (Supplementary Fig. S2B, C).

High NO is the cause of ob/ob mitochondrial dysfunction

To identify high matrix NO as an endpoint of mitochondrial dysfunction and obesity in leptin deficiency, we explored O_2 uptake in *ob/ob* WAT and liver mitochondria in the

Table 1. Production of Nitric Oxide in the *ob/ob* Mice

(A) NOS activity[a]

	Adipose tissue		*Liver*	
	Cytosol	*Mitochondria*	*Cytosol*	*Mitochondria*
Control	38±3	73±1	47±2	37±3
ob/ob	69±1[b]	220±2[c]	117±5[b]	154±4[c]

[a]Activity was measured by the conversion of ^{3}[H]L-arginine to ^{3}[H]L-citrulline and expressed in pmol NO/(min·mg of protein).
[b]$p<0.02$; [c]$p<0.001$; $n=4$.
NOS, nitric oxide synthase.

(B) Ex vivo *nitric oxide release by isolated mitochondria*[a]

	Liver
	Mitochondria
Control	6±1
ob/ob	27±2[b]

[a]Activity was measured with the NO sensor ISONOP 3020 and expressed in pmol NO/(min·mg of protein).
[b]$p<0.02$; $n=3$.

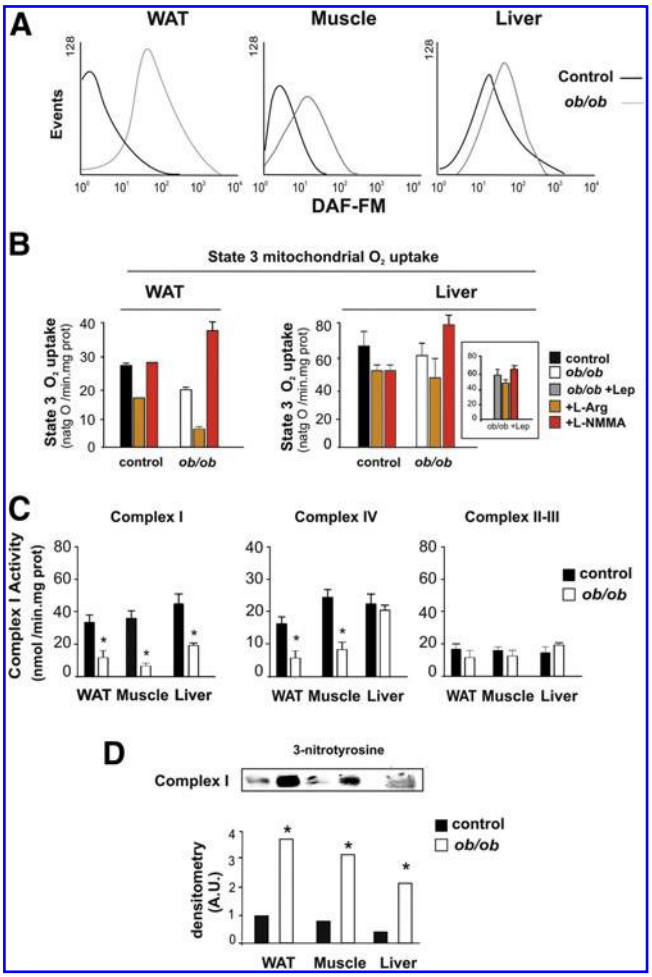

FIG. 3. High NO reduces oxygen uptake and nitrates *ob/ob* mitochondria in metabolic tissues. (A) Flow-cytometric histograms with mitochondria isolated and purified from WAT muscle and liver stained with DAF-FM; bars represent median peak fluorescence of the populations (mean ± SEM, $n = 5$); $^*p < 0.05$ *versus* control. **(B)** State 3 O_2 uptake of purified mitochondria from controls and *ob/ob* mice measured at 220 μM O_2, with malate/glutamate and adenosine diphosphate ($n = 3$–8); inset shows liver measurements with leptin treatment. **(C)** Electron transfer rate of mitochondrial complexes was spectrophotometrically measured in submitochondrial particles. $^*p < 0.05$ *versus wt* C57BL/6. **(D)** Nitrated proteins in mitochondrial complexes isolated by electrophoresis from metabolically active tissues were identified using an anti-3-nitrotyrosine antibody. $^*p < 0.05$ *versus wt* C57BL/6.

presence of NOS substrate L-arginine (L-Arg) and NOS inhibitor L-NMMA (Fig. 3B). Effects of NO on mitochondrial oxidative rate are approximately linear up to 0.6 μM NO (42). In these conditions, the sum of percentage variations of O_2 uptake with substrate and inhibitor reflects the NO steady-state concentration (mtNOS functional activity index) (14). mtNOS functional activity index was increased by one- to fourfold in *ob/ob* mice, being proportional to tissue DAF fluorescence in Figure 3A (in %; mean ± SEM, WAT: controls 42 ± 3 and *ob/ob* 160 ± 12, $n = 3$; liver: controls 22 ± 2 and *ob/ob* 53 ± 4, $n = 6$, $p < 0.05$). In addition, we found that *ob/ob* mitochondrial complex I activity was reduced by 50%–75% in WAT, muscle, and liver (Fig. 3C). Complex IV activity was reduced by about the same magnitude, but only in the mitochondria from *ob/ob* WAT and muscle. Cytosolic nNOS may as well contribute to nitration of mitochondrial complexes. It is, however, noteworthy that in *ob/ob*, NO is preferently driven to mitochondria (Table 1).

A key point of this study is whether the excess of mitochondrial NO and $ONOO^-$ anion causes the dysfunction in *ob/ob* mice (17) by the nitration of mitochondrial components (44). We therefore tested whether the decrease in complex I and IV activity in the absence of nNOS substrate or inhibitor represents stable modifications of mitochondrial components by nitrative stress in *ob/ob* mice (Supplementary Fig. S1). Western blotting with an anti-3-nitrotyrosine antibody revealed intense nitration at complex I in *ob/ob* mitochondria from WAT, liver, and muscle (Fig. 3D).

The nitration of WAT complex I in *ob/ob* mice that is associated with low complex I activity (the "complex I syndrome") (5, 16) was almost completely prevented by prior leptin administration (Fig. 4A). The maintenance of a normal electron transfer rate by leptin is in agreement with the normalization of basal metabolic rate of WAT in the *ob/ob* mice (Fig. 4B). Complex I is made up of >40 components, and the most nitrated components detected in *ob/ob* were the 75-kDa NDUFSI and the 39-kDa NDUFA9, which facilitate electron transfer from NADH to flavin adenine dinucleotide (Fig. 4C) (22). Likewise, reestablishment of complex I by leptin modifies the mitochondrial phenotype. Mitochondria from *ob/ob* mice are larger and had fewer cristae than controls, and this phenotype was reversed by leptin administration (Fig. 4D).

Leptin drives fatty acid metabolism through mitochondrial NO

To identify a functional signal link between leptin and mitochondrial NO, we knocked down the expression of the leptin receptor in normal adipocytes by transfection with ObRb siRNA. ObRb-deficient adipocytes with leptin resistance became enlarged and exhibited colocalization of NO with mitochondria, and lipid-confluent vacuoles were similar to *ob/ob* cell phenotype (Fig. 5A). Accordingly, leptin addition to adipocytes abolished the NO signal and concomitantly reduced cell lipid content. This fat reduction and the resulting cell shrinkage (37) were similar to that obtained by silencing nNOS and were accompanied by the relocation of mitochondria from the periphery to the center of the cells (Fig. 5A). Next, we compared the effects of leptin and mitochondrial NO on fat metabolism in the studied cells (Fig. 5B). Under basal conditions, ^{3}[H]palmitic acid uptake was similar between normal and *ob/ob* adipocytes; however, uptake was augmented in control cells upon leptin treatment. In addition, palmitic acid uptake was increased in *ob/ob* adipocytes treated with leptin or transfected with nNOS siRNA alone or in combination with leptin treatment (Fig. 5B). The basal rate of palmitic oxidation was similar between control and *ob/ob* cells, thus revealing a marked reduction in the rate of β-oxidation in the deficient adipocytes under conditions of high fatty acid availability. Adipocytes expressing ObRb siRNA and high NO had a reduced rate of palmitic acid oxidation (10%–20% of the basal value) with or without leptin. Conversely, nNOS deficiency and/or leptin administration tripled the rate of palmitic oxidation in *ob/ob* adipocytes, thus indicating the presence of a common mechanism for relieving

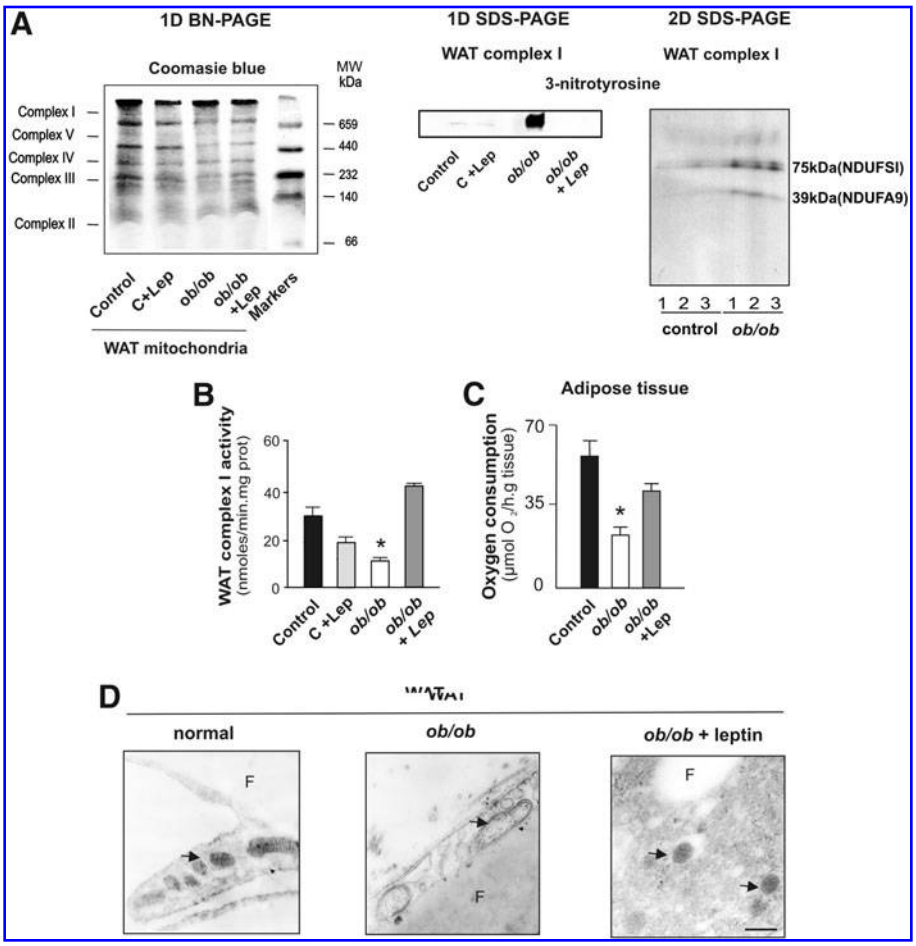

FIG. 4. Leptin protects *ob/ob* mitochondria from NO nitration of complex I and structural changes. (A) On the *left*, staining of mitochondrial complexes from adipose tissue in controls and obese mice with Coomassie blue (1D) is shown. In the *middle*, complex I nitration from *ob/ob* as detected with an anti-3-nitrotyrosine antibody and reversed by *in vivo* leptin administration is shown. On the *right*, 2D sodium dodecyl sulfate of complex I isolated of three *ob/ob* and three controls is shown. Blue native electrophoresis of the nitrated band in Figure 3D was utilized to detect nitration of complex I components. **(B)** Complex I activity of adipose tissue from mitochondria of controls and *ob/ob* mice treated with leptin *in vivo*. $*p < 0.05$ *versus wt* C57BL/6. **(C)** Leptin restored oxygen uptake of 5–10 mg sliced adipose tissue polarographically measured in phosphate-buffered saline (pH 7.4) with 5 m*M* glucose under normal atmosphere at 37°C ($n = 4$). Bars are mean ± SEM; $n = 7$; $*p < 0.05$ *versus* controls. **(D)** Electron microscopy shows structural differences in WAT mitochondria from normal, *ob/ob*, and *ob/ob* after leptin treatment (representative of three experiments; F, fat; *arrows*, mitochondria; bar = 1 μm).

the NO-dependent inhibition of β-oxidation. This inhibition and the resultant nonoxidized acetyl-CoA were evidenced by a concomitant increase in fatty acid synthesis by nNOS knockdown or leptin treatment (Fig. 5B).

Leptin restored the glycemic control and increased the metabolic rate of *ob/ob* mice (Supplementary Fig. S3A, B). Administration of leptin or NOS inhibitor L-N^Gnitroarginine methylester arginine (L-NAME) similarly interrupted the weight gain of *ob/ob* mice: at the end of the experiment (12 days), the weight difference between untreated and treated *ob/ob* mice was 23 ± 2 g or ~207 cal (9 cal/g), whereas the difference in food intake was 34.6 ± 3 g (3 cal/g) or 107 cal, demonstrating that ~50% of cumulated fat is due to mitochondrial dysfunction (Supplementary Fig. S3C, D).

Phospho-AMPK inhibits NOS within mitochondria

Leptin activates 5′-AMPK in skeletal muscle (33) and WAT (32) through the tumor suppressor LKB1 protein kinase (46). AMPK is a heterotrimeric enzyme that senses the energy status of the cell (7, 33) and functions as a regulator of cellular metabolism (20, 28, 48). AMPK also promotes fatty acid oxidation (37) and high O_2 utilization in response to a reduction in the ATP/AMP ratio by phosphorylating key enzymes of the intermediary metabolism (37, 47). In addition, AMPK and NO have opposite effects on respiration (28, 42). Thus, we investigated AMPK as the link between the effects of leptin and inhibition of mitochondrial nNOS. First, we observed that p-AMPK is normally expressed in the mitochondria of C57BL/6 *wt* mice. Conversely, *ob/ob* mitochondria are almost devoid of mitochondrial and cytosolic p-AMPK in WAT and liver, whereas the kinase is present in the cytosol in its nonphosphorylated form (Fig. 6A). Leptin increased the levels of cytosolic and mitochondrial p-AMPK in WAT and liver tissue of the obese mouse group (Fig. 6A). These data were also supported here by the *ex vivo* findings that recombinant p-AMPK enters the energized *ob/ob* mitochondria, whereas unphosphorylated AMPK is not able to enter the organelles (Fig. 6B). In this context, p-AMPK import was promptly followed by a significant reduction in the NO-DAF signal in mitochondria (Fig. 6C). nNOS has consensus sequences for AMPK and can be phosphorylated by this kinase. Stephens *et al.* have reported a parallel effect of p-AMPK on the phosphorylation of muscle nNOSμ and acetyl-CoA-carboxylase in human skeletal muscle (47). We observed that phosphorylation by p-AMPK inhibits nNOS activity by increasing the K' for L-Arg from 19.8 to 37.8 μM. Thus, the effect of P-AMPK on nNOS kinetics is opposite to that of p-Akt2 ($K' = 12.3\ \mu M$) (14) (Fig. 6D).

The ob/ob phenotype is due to a low p-AMPK/pAkt2 ratio

We previously reported that hyperinsulinemia increases mitochondrial p-Akt2, which activates the neuronal mtNOS

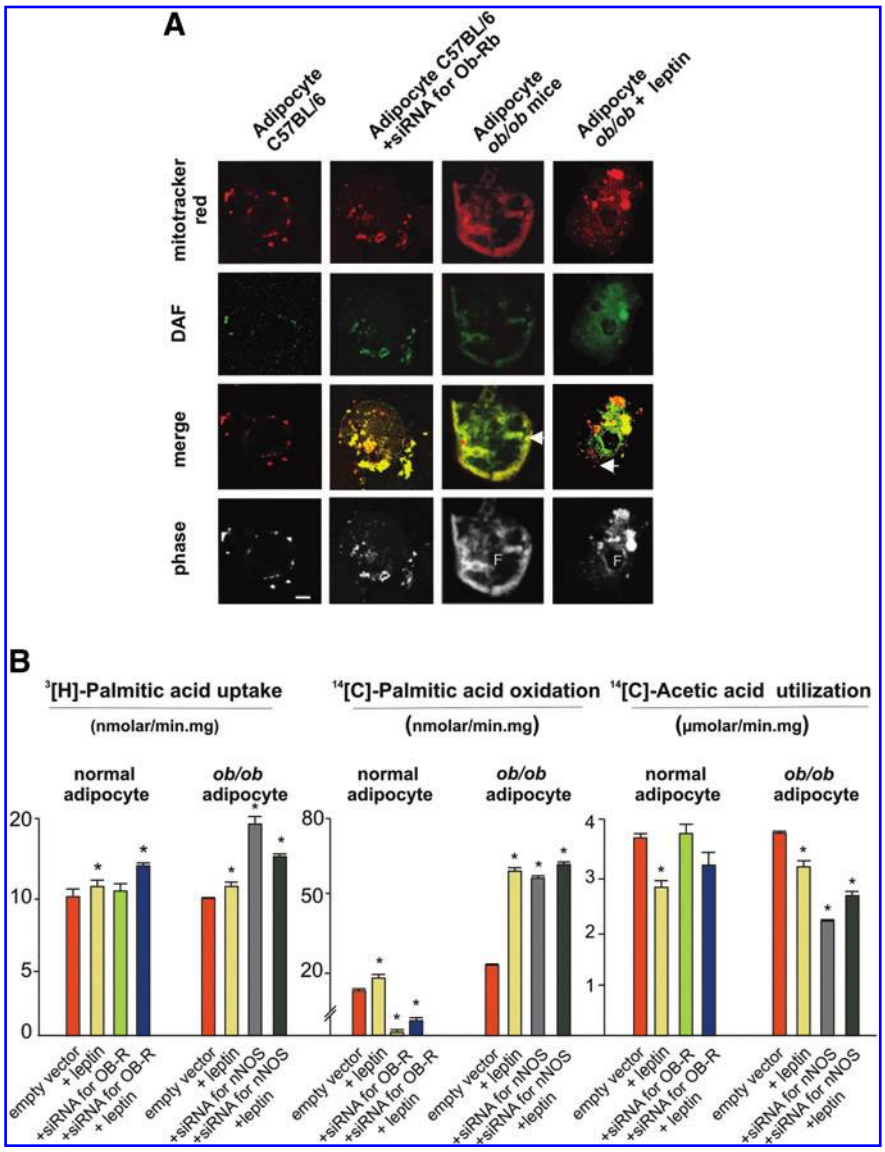

FIG. 5. Leptin drives fat metabolism through mitochondrial NO in adipocytes. (A) Mitochondria were detected by confocal microscopy, as in Figure 2. *First lane* shows control adipocytes. In the *second lane*, control adipocytes were transfected with 10 μg Ob-Rb siRNA. An increase of mitochondrial NO was achieved 24 h later. In the *third lane*, the image shows NO signal in mitochondria from *ob/ob* cells (*arrows*), and in the *fourth lane*, the signal was abolished by 100 ng/ml leptin. **(B)** The regulation of fatty acid metabolism by leptin and NO was compared in normal and ob/ob adipocytes by scintillation counting. For fatty acid uptake, cells were incubated with 1 μCi/ml ^{3}[H]-palmitic acid; β-oxidation was measured with 1 μCi/ml ^{14}[C]-palmitic acid and fatty acid synthesis was measured with 0.67 μCi/ml $^{1-14}$[C]-acetic acid. Bars are means ± SEM ($n = 8$); *$p < 0.05$ *versus* controls; *white bar* = 30 μm.

isoform by phosphorylating Ser^{1412} in the C-terminal domain with subsequent mitochondrial NO release (15). In the present study, the decrease of p-AMPK in the adipocytes of *ob/ob* mice was accompanied by a reciprocal increase of p-Akt2 and p-nNOS^{1412}, the active NO-producing mitochondrial isoform; the imbalance was corrected by *in vivo* leptin administration (Fig. 7A). An antagonistic relationship between p-AMPK and p-Akt2 has been reported, wherein p-AMPK dephosphorylates Akt2 and reduces Akt2 activity (25), and conversely, Akt phosphorylates AMPK at Ser^{485} and reduces AMPK activity (21). We observed here that the absence of p-AMPK in *ob/ob* mice is accompanied by a reciprocal increase in p-Akt2 in adipose cell lysates and mitochondria. In these mice, mitochondrial NOS is highly phosphorylated at Ser^{1412}, an effect that is dependent on the presence of p-Akt2. Similarly, experimental inhibition of AMPK by expressing an siRNA targeting the catalytic AMPK or by the pharmacological inhibitors Ara-A or CC increased p-Akt2/NO and fat occupancy and changed normal adipocytes into *ob/ob*-like cells (Fig. 7A). Conversely, transfection of *ob/ob* mice with Akt2 siRNA or supplementation with the AMPK stimulators AICAR and A769662 decreased p-Akt2/NO and reversed the *ob/ob* phenotype by limiting fat accumulation. In all cases, the p-AMPK/p-Akt2 ratio linked kinase predominance to the metabolic status of the cells (Fig. 7C).

Discussion

Several lines of evidence support the existence of mitochondrial dysfunction in insulin-resistant states (50). In this condition, energy failure is attributed to insufficient biogenesis (24), excessive mitochondrial fission (49), and reduced amounts of adiponectin in the visceral adipocytes (23). In general, these alterations involve defective AMPK phosphorylation (sensitive to leptin–LKB axis) and poor AMPK-dependent activation of PCG-1 coactivator, a masterpiece in mitochondrial repopulation (24).

The relationship between NO and mitochondrial function is centered upon the modulation of the oxidative rate (Supplementary Fig. S1) (1, 42). We demonstrate herein that

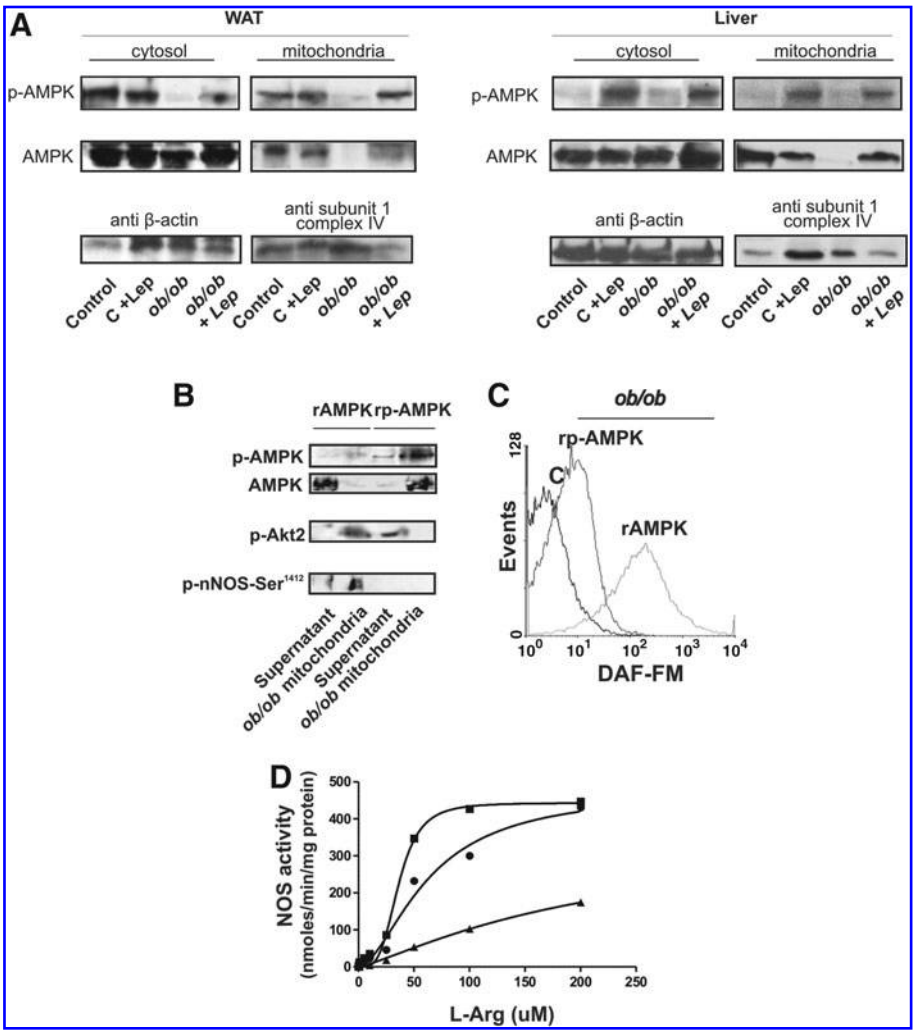

FIG. 6. Leptin–AMP-dependent kinase (AMPK)–mitochondrial NOS axis in the origin of obesity. **(A)** Western blotting of AMPK and p-AMPK in WAT and liver from the *ob/ob* mice ($n=6$). **(B)** To test kinase internalization, 50 μg/ml of *ob/ob* WAT mitochondria was treated with proteinase K as in Figure 1 and exposed to 2 μg recombinant p-AMPK or dephosphorylated AMPK for 30 min *in vitro*; western blot shows the effects p-AMPK on the p-Akt2 level and the consequent phosphorylation of nNOS in Ser^{1412} in mitochondria ($n=3$). **(C)** Modulation of mitochondrial NO in the isolated and purified *ob/ob* organelles exposed to exogenous recombinant rp-AMPK and nonphosphorylated rAMPK. C, control mitochondria ($n=3$). **(D)** Cooperative nNOS kinetics with L-arginine (L-Arg) after phosphorylation with recombinant p-Akt2 and p-AMPK and 2 m*M* ATP (*circles*, nonphosphorylated; *squares*, p-Akt2; *triangles*, p-AMPK; $n=3$); NOS activity was measured with 0.1 μM [^{3}H]L-arginine by triplicate.

overexpression and translocation of nNOS to mitochondria plays a key role in mitochondrial dysregulation of MS linked to leptin deficiency and insulin resistance. NO increases superoxide anion to yield $ONOO^-$ (41, 42). Thereby, electron transfer inhibition by NO in *ob/ob* depended in part on COX inhibition and in part on complex I inhibition mostly because of significant nitration of 39- and 75-kDa components. Although NO can increase mitochondrial biogenesis (36), organelles with extensive nitrosative damage are probably not renovated because of critical downregulation of biogenesis by low adiponectin and AMPK levels (43). The possibility that diabetes is associated with increased nitrosative stress is supported by recent detection of increased nytrotirosine plasma levels in type 2 diabetes patients. Nitrotyrosine formation is detected in diabetic patients during an increase of postprandial hyperglycemia (38).

As shown here by different methods, mitochondrial NO detection increases by fourfold at abnormal leptin–insulin signaling. Subcellular localization of NO synthases is an important regulatory mechanism for NO signaling. Spatial confinement of the different NO synthase isoforms allows NO to have independent and even opposite effects (3). In parallel to mitochondrial nNOS activation, hyperglycemia induces vascular dysfunction by inactivation of eNOS isoform leading to reduced NO availability. As such, local regulation of effector molecules is a central mechanism by which NO exerts biological activity (3).

It is noteworthy that increased mitochondrial NO should favor pyruvate, acetylCoA, and NADH accumulation. By resetting the electron transfer rate, mitochondrial NO controls the partition between substrate oxidation (β-oxidation and glucose oxidation) and substrate deposit and accumulation (fatty acid, triacylglycerol, and glycogen synthesis; Fig. 8). By applying NO reduction of respiratory rate of 10 μmol O_2/(mg·min) or 1.73 mol O_2/day (as observed in *ob/ob* in Fig. 3B) to a young lean mice with 4 g fat and $\sim$30 mg mitochondria/g fat, and considering the stoichiometry of β-oxidation, we estimate that 72.5 g palmitate should not be oxidized at adulthood, allowing to $\sim$60 g fat accumulation. This assumption agrees with the measured weight difference between 9-month-old *ob/ob* and lean mice (53 g; Supplementary Fig. S3D). In accord, release of the NO inhibition by siRNA nNOS reproduced leptin effects and encompassed O_2 utilization of available adipose acetyl-CoA to maximal β oxidation rate and minimal fatty acid synthesis (Fig. 5B).

Matrix NO and mtNOS are tightly linked by insulin, leptin, and thyroid hormones to different metabolic processes. We demonstrate here that leptin modulates mitochondrial effects of NO by different mechanisms. First, leptin deficiency increases transcriptional activity of nNOS gene. We previously

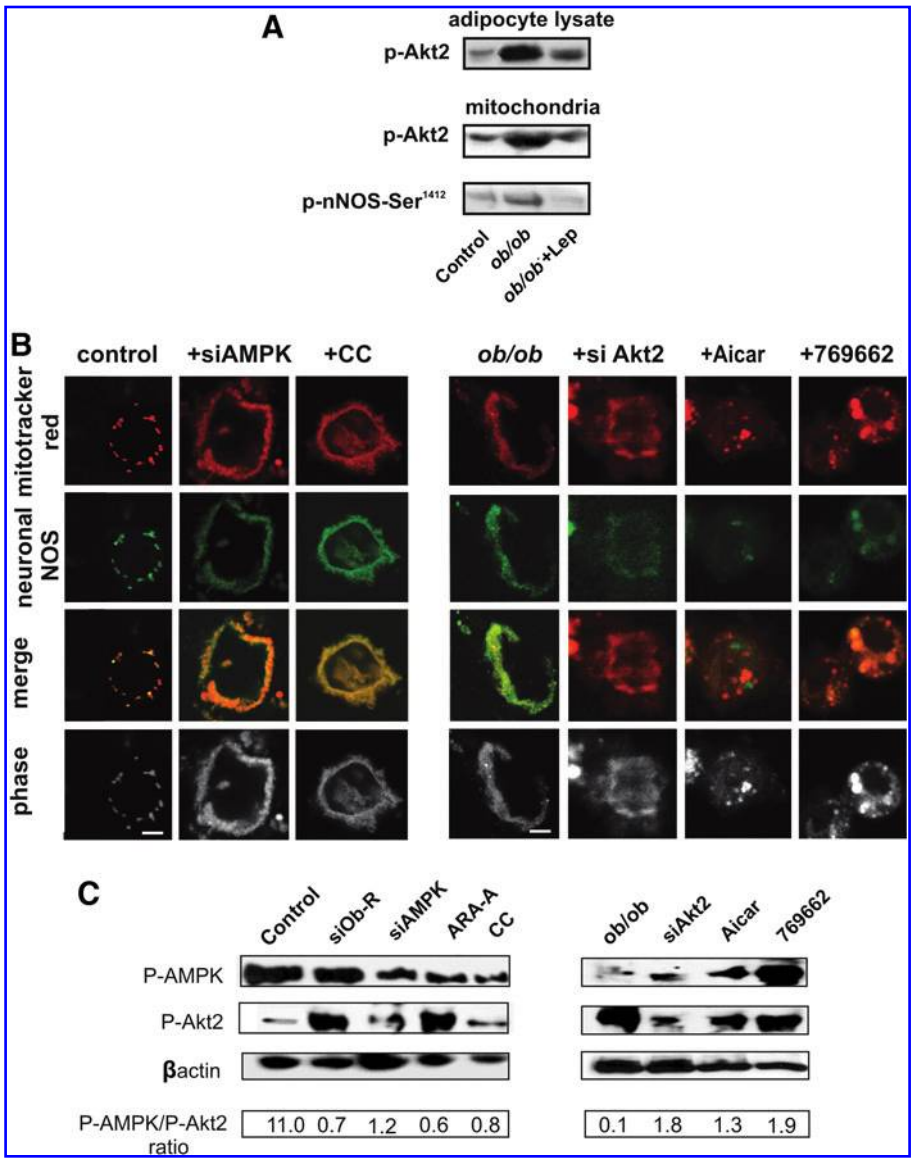

FIG. 7. Mitochondrial AMPK/Akt2 ratio sets NO level and adipocyte phenotype. (A) Expression of p-Akt2 in *ob/ob* adipocytes devoid of p-AMPK; western blots were performed using specified antibodies. **(B)** Control adipocytes were transfected with 10 μg AMPK siRNA or incubated with AMPK inhibitors Ara-A (1 m*M*) or CC (50 μ*M*); *ob/ob* adipocytes were transfected with 10 μg Akt2 siRNA or supplemented with AMPK stimulators 769662 (300 μ*M*) or AICAR (1 m*M*); in all cases, cells were analyzed by confocal microscopy as in Figure 2. *White bar* = 30 μm. **(C)** Western blot shows p-AMPK/p-Akt2 ratio; all data are representative of triplicate samples in two experiments.

reported that hypothyroidism similarly induces a high expression of nNOS (9, 16); as a certain degree of hypothyroidism is present in *ob/ob*, it could contribute to transcriptional effects of leptin deficiency. Second, NOS activity is controlled by the leptin–p-AMPK pathway in mitochondria (Figs. 6 and 7). By reducing mtNOS activity and NO yield, leptin and p-AMPK accelerate fatty acid oxidation, causing an antiobese effect; the decreased fat accumulation is contributed by AMPK phosphorylation of acetyl-CoA-carboxylase (28, 47) and inhibition of fatty acid synthetase in adipose, muscle, and liver tissues (37). In addition to leptin, the stimulatory effects on AMPK and mitochondrial respiration are supported by adiponectin (25). In contrast, Akt2 promotes lipogenesis by different effects related to insulin. Prolonged insulin effects produce muscle mitochondrial dysfunction by activating nNOS *via* p-Akt2 (14). In the present study, we have shown that obesity with mitochondrial dysfunction in *ob/ob* mice is associated with high p-Akt2 and phospho-nNOS levels in the mitochondria (Figs. 5 and 6). Other insulin effects can contribute to fat deposition in the liver, such as inhibition of peroxisome proliferator activated receptor gamma coactivator1-alpha and reduction of 3′5′-cAMP (27).

Finally, it is worth noting here that the balance between p-AMPK and p-Akt2 controls NO production (Fig. 7) and significantly affects mitochondrial physiology and pathology. This balance determines the physiological oxygen uptake and metabolic rate in different conditions of energy intake and expenditure (Fig. 8). In addition, the persistent NO-dependent production of superoxide leads to oxidation of proteins and lipids and to the nitration of complex I with progressive mitochondrial dysfunction (complex I syndrome) (5), a hallmark of MS and diabetes (2, 30). Moreover, NO and O_2 species activates inflammatory pathways, a secondary effect consistent with persistently low-level inflammation of fat tissues.

Obesity and diabetes are multifactorial entities with considerable interrelationship between the metabolic participants. Mitochondrial NO could be a common final effector of leptin–insulin signaling pathways. Considering the impending advance of obesity, regulation of nNOS trafficking

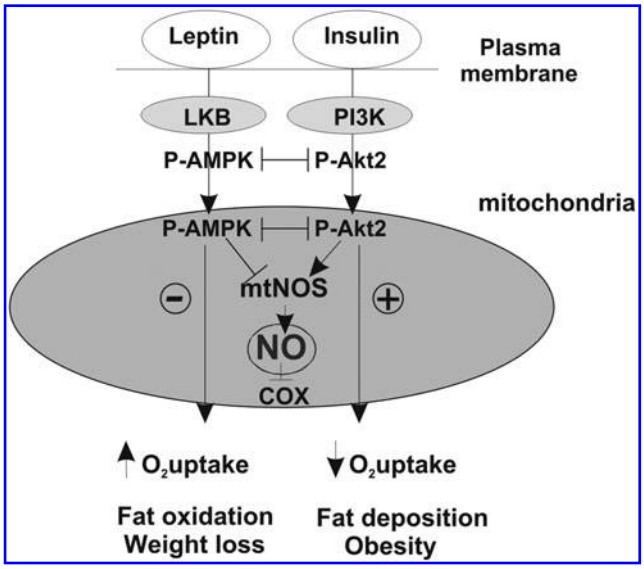

FIG. 8. Model illustrating the regulation of body weight by mitochondrial NO. Endocrine–paracrine effects of insulin and leptin depend on the relative activation and translocation to mitochondria of phosphorylated AMPK and Akt2. At low or no NO levels (high p-AMPK/p-Akt2 ratio), the electron transfer chain is released and acetyl-CoA is mostly oxidized. At high NO levels (low p-AMPK/p-Akt2 ratio), cytochrome oxidase is inhibited and acetyl-CoA is displaced to synthesize fatty acids, which causes fat accumulation and obesity.

may be applied to therapeutic approaches for these metabolic disorders.

Methods

Mice

Male *ob/ob* and C57BL/6 *wt* mice (6–9 months old) from Jackson Labs were divided in groups into three treatment groups: no intervention, mouse recombinant leptin (1 mg/kg intraperitoneal for 4 days) (39) (Sigma Chemical Co.), or L-NAME in the drinking water. NIH criteria for animal research were followed and protocols were approved by the university hospital. Mitochondria were isolated from homogenized tissue by differential centrifugation and further purification was done with Percoll gradients (15). The purity of isolated mitochondria was confirmed by flow cytometry and mitotracker staining, with >98% of the particles being positive with respect to the unstained population, thus indicating minimal contamination with other subcellular fractions (Supplementary Fig. S4A). Only trace amounts of cytosolic proteins (<5% lactic dehydrogenase) were detected in the isolated mitochondria, indicating a low index of contamination. Expression of nNOS, AMPK-α, p-AMPK (Thr 172), Akt2, and p-Akt2 (Thr 308) was assessed by specific immunoblotting.

Mitochondrial NO production

NO production in isolated mitochondria was measured by flow cytometry using 10 μM DAF-FM and 0.5 μM MitoTracker Red 580 in 1× phosphate-buffered saline (PBS) with 3 mM L-NMMA. Fluorescence was measured with an Ortho Cytoron Absolute Flow Cytometer (Johnson & Johnson) (29). Total WAT RNA was extracted with Trizol, and real-time PCR was performed in standard conditions.

Systemic O_2 consumption

Systemic O_2 consumption was measured in an open circuit with an O_2 analyzer and CO_2 analyzer set in series (40). Consumption was calculated at room air temperature and barometric pressure by measuring flux through the chamber and expired fraction of effluent O_2 and CO_2. Expired gases were normalized to standard temperature/pressure and dry weight, and O_2 uptake was normalized to lean body mass (as ml O_2/min body mass$^{2/3}$).

Tissue and mitochondrial O_2 utilization and electron transfer activity

O_2 uptake was polarographically measured with a Clark-type electrode (13). According to pioneer studies of Chance, mitochondria can be analyzed in different states. In the presence of substrate and O_2, state 4 O_2 uptake was determined with 6 mM malate/6 mM glutamate; malate oxidation to oxalacetate provides electrons to be ultimately transferred to O_2. Addition of glutamate was used to avoid interferences given by concomitant succinate oxidation (12). State 3 O_2 uptake was measured by the further addition of 0.2 M adenosine diphosphate. The respiratory control ratio (state 3/state 4) ranged from 4 (adipose) to 7 (liver). To assess the effects of NO, mitochondria were incubated with 0.3 mM L-Arg alone or with 3 mM L-NMMA for 5 min at 37°C. The percentage of mitochondria functional activity was calculated as the % of reduction of state 3 O_2 uptake with L-Arg plus the % of increase of state 3 O_2 uptake with L-NMMA (14). Complex I activity (NADH: ubiquinone reductase) was measured in submitochondrial particles (15) by the rotenone-sensitive reduction of 50 μM 2,3-dimethoxy-6-methyl-1,4-benzoquinone with 1 mM KCN and 200 μM NADH as the electron donor. Measurements were collected at 340 nm with a Hitachi U3000 spectrophotometer (Hitachi). The activity of complexes II–III was determined by cytochrome *c* reduction at 550 nm. Cytochrome oxidase activity (complex IV) was determined by cytochrome *c* oxidation at 550 nm (ε_{550}, 21 mM^{-1} cm^{-1}); the reaction rate was measured as the pseudo-first order reaction constant (k') and expressed as k'/(min·mg of protein) (15).

Blue native polyacrylamide gel electrophoresis

Blue native polyacrylamide gel electrophoresis was carried out according to Schägger (45). Samples were loaded onto a nondenaturing 4%–15% gradient gel, using the previously described electrophoresis buffers and conditions.

Primary fat cell isolation

Fat pads were sliced into 3-mm pieces and resuspended in buffer with 5 mM glucose, 2.5% bovine serum albumin, and 0.5 mg/ml collagenase (Sigma Chemical Co.) (31). Fat was digested for 45–60 min, and the released adipocytes were harvested by centrifugation. Cells in the upper phase were collected, washed, and resuspended in 0.15 M PBS.

siRNA transfection of white adipose cells

Adipocytes were transfected with siRNAs targeting nNOS (GenScript), OB-Rb (sc: 36116; Santa Cruz Biotechnology) (Supplementary Fig. S4B), Akt2 (Santa Cruz Biotechnology), or AMPK α1 (sc: 29674; Santa Cruz Biotechnology) using Lipofectamine (Invitrogen) in Opti-MEM medium. Transfected cells were incubated at 37°C in a CO_2 incubator for 18–24 h with or without 100 ng/ml (submaximal leptin dose in *ob/ob* adipocytes; Supplementary Fig. S4B). The sequence of the nNOS siRNA was designed according to the structure of mouse nNOS g.i. 16258811, as shown in Supplementary Figure S4D.

Translocation of AMPK to mitochondria and modulation of nNOS

Two milligrams of mitochondrial protein was incubated with 2 m*M* ATP, 2 m*M* NADH, and a recombinant cAMP protein kinase catalytic subunit protein (ab 56268; Abcam, Inc.) or a dephosphorylated isoform. The resulting mixture was incubated with acid phosphatase for 30 min and then centrifuged at 10,000 *g* for 10 min to separate mitochondria. The pellets were resuspended and incubated with 50 μg/ml proteinase K, and western blots were performed with different antibodies. Flow-cytometric analysis of isolated mitochondria incubated with phosphorylated or nonphosphorylated AMPK kinase and dyed with DAF-FM was performed. To test the effects of mitochondrial NOS on a related adipocyte phenotype, p-AMPK was experimentally decreased in controls with the compounds CC or Ara-A or increased in *ob/ob* cells by supplementation with AICAR or compound 769662, or by transfection with Akt2 siRNA. The effects of these compounds were then analyzed by confocal microscopy.

NOS activity in vitro *and* in vivo

NOS activity in cytosol and mitochondrial fractions of liver and adipose tissues from control and *ob/ob* mice was determined by conversion from ^{3}H L-Arg to ^{3}H L-citrulline (14) in 50 m*M* potassium phosphate buffer, pH 7.4, in the presence of 100 μ*M* L-Arg, 0.1 μ*M* [^{3}H]-L-arginine (NEN), 0.1 m*M* NADPH, 0.3 m*M* $CaCl_2$, 0.1 μ*M* calmodulin, 10 μ*M* tetrahydrobiopterin, 1 μ*M* flavin adenine dinucleotide, 1 μ*M* flavin mononucleotide, 50 m*M* L-valine, and 1 mg/ml protein. Specific activity was calculated by subtracting the remaining activity in the presence of the NOS inhibitor 5 m*M* L-NMMA or 2 m*M* ethylene glycol tetraacetic acid.

In vitro assay was performed with recombinant His-tagged nNOS protein purified from *Escherichia coli* bacteria that had been transiently transfected with a pcDNA 3.1 vector containing the nNOS cDNA sequence. NOS activity of the purified protein alone or in the presence of active human recombinant Akt2 (phosphorylated at Ser^{473} and Thr^{308}) or active human recombinant AMPKα1 (phosphorylated at Thr^{172}) was evaluated by citrulline assay (14).

Production of NO by isolated mitochondria in liver was corroborated by potenciometric recording with an NO-sensitive electrode (ISO-NOP 3020; World Precision Instruments). Determinations were done in 50 m*M* potassium phosphate/valine buffer (pH 7.4) with 100 m*M* L-Arg, 10 μ*M* superoxide dismutase mimetic manganese(III) tetrakis 4-benzoic acid)porphyrin (9) (Cayman Chemical), 5 m*M* succinate, and 1 m*M* $CaCl_2$.

Fatty acid metabolism

Adipocytes were incubated with [^{3}H]palmitic acid, and samples were counted to measure fatty acid uptake. For β-oxidation, isolated adipocytes were distributed into tubes containing Whatman filter paper soaked in NaOH and 200 nCi/ml [^{14}C]palmitic acid. The tubes were sealed and incubated for 2 h; then, 10 N HCl was added to release [^{14}C]CO_2, which was detected by scintillation counting of the filter paper. Fatty acid synthesis was evaluated using a scintillation counter (Winspectral 1414; Wallac) to measure the incorporation of [$^{1\text{-}14}$C] acetyl-CoA into lipids extracted with chloroform:methanol (2:1 ratio). Radioactive chemicals were purchased from Perkin Elmer Life and Analytical Sciences.

Confocal microscopy

Ob/ob and control adipocytes previously transfected with siRNA nNOS and siRNA Ob-Rb, respectively, were incubated with 10 μ*M* DAF and 50 n*M* Mitotracker for 45 min at 37°C in a CO_2 incubator. Then, 10^3 cells were fixed in 4% paraformaldehyde in 0.15 *M* PBS (pH 7.4) and mounted on glass slides using Vectashield mounting medium. The staining was examined with a fluorescence microscope equipped with a confocal laser scanning system (29) (Nikon C1; Nikon Instruments, Inc.).

Immunoelectron microscopy

Purified mitochondria were fixed with paraformaldehyde–glutaraldehyde and embedded in LR White. Immunocytochemistry was performed using anti-C-terminal nNOS (1095–1289), and grids were counterstained with 1% uranyl acetate. Nonspecific background was blocked with normal goat serum in PBS. The positive control was performed against the 39-kDa subunit of complex I (inner membrane marker), and the negative control was performed in the absence of a primary antibody. Specimens were observed using a Zeiss EM-109-T transmission electron microscope.

Statistics

Values are reported as mean ± SEM. Data were compared by analysis of variance, Dunnett's *post hoc* test, and two-tailed Student's *t*-test, and significance was accepted at $p < 0.05$.

Acknowledgments

The authors thank Margarita López for electron microphotographs, Eduardo Spinedi for help and advice with adipocyte preparations, Marcos Barboza for flow-cytometric determinations, Pablo Docampo for help with image quantification, Dennis Stuehr for cloning nNOS, Selva Cigorraga for kindly providing the AMPK modulators Ara-A, CC, Aicar, and 769662 compounds, and Alvaro Estévez for reading the manuscript and for helpful discussions. This work was supported by the Agencia Nacional de Promoción Científica y Tecnológica (Foncyt) grants PICT 1625, PICT 21461, and PICT 34785 (to M.C.C. and J.J.P.), University of

Buenos Aires (Ubacyt M058), Conicet (PIP 5495 to M.C.C.), and Fundación Pérez Companc, Buenos Aires, Argentina, and a training grant from the Fundación Florencio Fiorini (to F.B.).

Author Contribution

P.V.F., M.C.C., and J.J.P. designed the study; P.V.F., S.H., F.B., and J.G.P. performed experiments; Y.A. performed the PCR experiment; P.V.F., M.C.C., and J.J.P. collected and analyzed data; A.G. prepared the adipocytes, provided mice, and gave conceptual advice; P.V.F., M.C.C., and J.J.P. wrote the manuscript; M.C.C. and J.J.P. equally contributed to this work.

Author Disclosure Statement

The authors declare that no competing financial interests exist.

References

1. Antunes F, Boveris A, and Cadenas E. On the mechanism and biology of cytochrome oxidase inhibition by nitric oxide. *Proc Natl Acad Sci U S A* 101: 16774–16779, 2004.
2. Araki E and Miyazaki JI. Metabolic disorders in diabetes mellitus: impact of mitochondrial function and oxidative stress on diabetes and its complications. *Antiox Redox Signal* 3: 289–291, 2007.
3. Barouch LA, Harrison RW, Skaf MW, Rosas GO, Cappola TP, Kobeissi ZA, Hobal IA, Lemmon CA, Burnett AL, O'Rourke B, Rene Rodriguez E, Huang PL, Lima JCA, Berkowitz DE, and Hare JM. Nitric oxide regulates the heart by spatial confinement of nitric oxide synthase isoforms. *Nature* 416: 337–340, 2002.
4. Boczkowski J, Poderoso JJ, and Motterlini R. CO-metal interaction: vital signaling from a lethal gas. *TIBS* 31: 614–621, 2007.
5. Boveris A, Carreras MC, and Poderoso JJ. The regulation of cell energetic and mitochondrial signaling by nitric oxide. In: *Nitric Oxide: Biology and Pathobiology*, edited by Ignarro LJ. San Diego: Academic Press, 2010, pp. 441–482.
6. Brown GC. Nitric oxide regulates mitochondrial respiration and cell functions by inhibiting cytochrome oxidase. *FEBS Lett* 369: 136–139, 1995.
7. Cantó C, Gerhart-Hines Z, Feige JN, Lagouge M, Noriega L, Milne JC, Elliot PJ, Puigserver P, and Auwerx J. AMPKregulates energy expenditure by modulating NAD1 metabolism and SIRT1 activity. *Nature* 458: 1056–1060, 2009.
8. Carreras MC, Converso PD, Lorenti AS, Barbich M, Levisman DM, Jaitovich A, Antico Arciuch VG, Galli S, and Poderoso JJ. Mitochondrial nitric synthase drives redox signals for proliferation and quiescence in rat liver development. *Hepatology* 40: 157–166, 2004.
9. Carreras MC, Peralta JG, Converso PD, Finocchietto PV, Rebagliati I, Zaninovich AA, and Poderoso JJ. Modulation of liver mitochondrial NOS is implicated in thyroid-dependent regulation of O_2 uptake. *Am J Physiol Cell Physiol* 281: H2282–H2288, 2001.
10. Carreras MC and Poderoso JJ. Mitochondrial nitric oxide in the signaling of cell integrated responses. *Am J Physiol Cell Physiol* 292: C1569–C1580, 2007.
11. Ceddia RB. Direct metabolic regulation in skeletal muscle and fat tissue by leptin: implications for glucose and fatty acids homeostasis. *Int J Obesity* 29: 1175–1183, 2005.
12. Chance B and Hagihara B. Activation and inhibition of succinate oxidation following adenosine diphosphate supplements to pigeon heart mitochondria. *J Biol Chem* 237: 3540–3545, 1962.
13. Estabrook RW. Mitochondrial respiratory control and the polarographic measurement of ADP:O ratio. In: *Methods in Enzymology*, edited by Estabrook RW and Pullman ME. New York: Academic Press, 1967, p. 41.
14. Finocchietto PV, Barreyro F, Holod S, Peralta JG, Franco MC, Méndez C, Converso PD, Estévez A, Carreras MC, and Poderoso JJ. Control of muscle mitochondria by insulin entails activation of Akt2-mtNOS pathway: implications for the metabolic syndrome. *PLoS ONE* 3: e1749, 2008.
15. Franco MC, Antico Arciuch VG, Peralta JG, Galli S, Levisman D, López LM, Romorini L, and Poderoso JJ. Hypothyroid phenotype is contributed by mitochondrial complex I inactivation due to translocated neuronal nitric oxide synthase. *J Biol Chem* 281: 4779–4786, 2006.
16. García-Ruiz I, Rodriguez-Juan C, Díaz-Sanjuan T, del Hoyo P, Colina F, Muñoz-Yagüe T, and Solis-Herruzo JA. Uric acid and anti-TNF antibody improve mitochondrial dysfunction in ob/ob mice. *Hepatology* 44: 581–591, 2006.
17. García-Ruiz I, Rodriguez-Juan C, Díaz-Sanjuan T, Martínez MA, Muñoz-Yagüe T, and Solis-Herruzo JA. Effects of rosiglitazone on the liver histology and mitochondrial function in ob/ob mice. *Hepatology* 46: 414–423, 2007.
18. Giulivi C, Poderoso JJ, and Boveris A. Production of nitric oxide by mitochondria. *J Biol Chem* 273: 11038–11043, 1998.
19. Haffner S and Taegtmeyer H. Epidemic obesity and the metabolic syndrome. *Circulation* 108*:* 1541–1545, 2003.
20. Hardie G. The AMPK-activated protein kinase pathway-new players upstream and downstream. *J Cell Sci* 117: 5479–5487, 2004.
21. Horman S, Vertommen D, Heath R, Neumann D, Mouton V, Woods A, Schlattner U, Wallimann T, Carling D, Hue L, and Rider MH. Insulin antagonizes ischemia-induced Thr^{172} phosphorylation of AMP-activated protein kinase α-subunits in heart via hierarchical phosphorylation of $Ser^{485/491}$. *J Biol Chem* 281: 5335–5340, 2006.
22. Iuso A, Scacco S, Piccoli C, Bellomo F, Petruzzella V, Trentadue R, Minuto M, Ripoli M, Capitanio N, Zeviani M, and Papa S. Dysfunctions of cellular oxidative metabolism in patients with mutations in the *NDUFS1* and *NDUFS4* genes of complex I. *J Biol Chem* 281: 10374–10380, 2006.
23. Iwabu M, Yamauchi T, Okada-Iwabu M, Sato K, Nakagawa T, Funata M, Yamaguchi M, Namiki S, Nakayama R, and Tabata M. Adiponectin and AdipoR1 regulate PGC-1a and mitochondria by Ca2 and AMPK/SIRT1. *Nature* 464: 1313–1319, 2010.
24. Jornayvaz FR and Shulman GI. Regulation of mitochondrial biogenesis. *Essays Biochem* 47: 69–84, 2010.
25. King TD, Song L, and Jope RS. AMP-activated protein kinase (AMPK) activating agents cause dephosphorylation of Akt and glycogen synthase kinase-3. *Biochem Pharmacol* 71: 1637–1647, 2006.
26. Knight ZA, Schot Hannan K, Greenberg ML, and Friedman JM. Hyperleptinemia is required for the development of leptin resistance. *PLoS ONE* 5: e11376, 2010.
27. Leavens KF, Easton RM, Shulman GI, Previs SF, and Birmbaun M. Akt2 is required for hepatic lipid accumulation in models of insulin resistance. *Cell Metab* 10: 405–418, 2009.
28. Long YC and Zierath JR. AMP-activated protein kinase signaling in metabolic regulation. *J Clin Invest* 116: 1776–1783, 2006.

29. López-Figueroa MO, Caamaño C, Morano MI, Rønn LC, Akil H, and Watson SJ. Direct evidence of nitric oxide presence within mitochondria. *Biochem Biophys Res Commun* 272: 129–133, 2000.
30. Lowell BB and Shulman GI. Mitochondrial dysfunction and type 2 diabetes. *Science* 307: 383–387, 2005.
31. Malide D. *Adipose Tissue Protocols. Methods in Molecular Biology*, vol. 155. New York: Springer, 2001, pp. 53–65.
32. Martínez-Agustin O, Hernández-Morante JJ, Martínez-Plata E, Sánchez de Medina F, and Garaulet M. Differences in AMPK expression between subcutaneous and visceral adipose tissue in morbid obesity. *Regul Pept* 163: 31–36, 2010.
33. Minokoshi Y, Kim YB, Peroni OD, Fryer LG, Müller C, Carling D, and Kahn BB. Leptin stimulated fatty-acid oxidation by activating AMP-activated protein kinase. *Nature* 415: 339–343, 2002.
34. Montague CT, Farooqi IS, Whitehead JP, Soos MA, Rau H, Wareham NJ, Sewter CP, Digby JE, Mohammed SN, Hurst JA, Cheetham CH, Earley AR, Barnett AH, Prins JB, and O'Rahilly S. Congenital leptin deficiency is associated with severe early-onset obesity in humans. *Nature* 387: 903–908, 1997.
35. Muoio DM and Lynis Dohm G. Peripheral actions of leptin. *Best Practice Res Clin Endocrinol Metab* 16: 653–666, 2002.
36. Nisoli E, Falcone S, Tonello C, Cozzi V, Palomba L, Fiorani M, Pisconti A, Brunelli S, Cardile A, Francolini M, Cantoni O, Carruba MO, Moncada S, and Clementi E. Mitochondrial biogenesis by NO yields functionally active mitochondria in mammals. *Proc Natl Acad Sci U S A* 101: 16507–16512, 2004.
37. Orci L, Cook WS, Ravazzola M, Wang MY, Park BH, Montesano R, and Unger RH. Rapid transformation of white adipocytes into fat-oxidizing machines. *Proc Natl Acad Sci U S A* 101: 2058–2063, 2004.
38. Pacher P, Obrosova IG, Mabley JG, and Szabó C. Role of nitrosative stress and peroxynitrite in the pathogenesis of diabetic complications. Emerging new therapeutical strategies. *Curr Med Chem* 12: 267–275, 2005.
39. Pelleymounter MA, Cullen MJ, Baker MB, Hecht R, Winters D, Boone T, and Collins F. Effects of the obese gene product on body weight regulation in ob/ob mice. *Science* 269: 540–543, 1995.
40. Peralta JG, Finocchietto PV, Converso PD, Schöpfer F, Carreras MC, and Poderoso JJ. The modulation of mitochondrial nitric oxide synthase and energy expenditure in rat cold acclimation. *Am J Physiol Cell Physiol* 284: H2375–H2383, 2003.
41. Poderoso JJ, Carreras MC, Lisdero C, Riobó N, Schöpfer F, and Boveris A. Nitric oxide inhibits electron transfer and increases superoxide radical production in rat heart mitochondria and submitochondrial particles. *Arch Biochem Biophys* 328: 85–92, 1996.
42. Poderoso JJ, Lisdero C, Schöpfer F, Riobó N, Carreras MC, Cadenas E, and Boveris A. The regulation of mitochondrial oxygen uptake by redox reactions involving nitric oxide and ubiquinol. *J Biol Chem* 274: 37709–37716, 1999.
43. Ren J, Pulakat L, Whaley Conell A, and Sowers JR. Mitochondrial biogenesis in the metabolic syndrome and cardiovascular disease. *J Mol Med* 88: 993–1001, 2010.
44. Riobó NA, Clementi E, Melani M, Boveris A, Cadenas E, Moncada S, and Poderoso JJ. Nitric oxide inhibits mitochondrial NADH:ubiquinone reductase activity through peroxynitrite formation. *Biochem J* 359: 139–145, 2001.
45. Schägger H. Blue native gels to isolate proteins complexes from mitochondria. *Methods in Cell Biol* 65: 231–244, 2001.
46. Shaw RJ, Kosmatka M, Bardeesy N, Hurley RL, Witters LA, DePinho RA, and Cantley LC. The tumor 17-suppressor LKB1 kinase directly activates AMP-activated kinase and regulates apoptosis in response to energy stress. *Proc Natl Acad Sci U S A* 101: 3329–3335, 2004.
47. Stephens TJ, Chen ZP, Canny BJ, Michell BJ, Kemp BE, and McConell GK. Progressive increase in human skeletal muscle AMPK-2 activity and ACC phosphorylation during exercise. *Am J Physiol Endocrinol Metab* 282: E688–E694, 2002.
48. Towler MC and Hardie DG. AMP-activated protein kinase in metabolic control and insulin signaling. *Circ Res* 100: 328–341, 2007.
49. Yoon Y, Galloway CA, Jhun BS, and Yu T. Mitochondrial dynamics in diabetes. *Antioxid Redox Signal* 14: 939–957, 2010.
50. Zorzano A, Liesa M, and Palacín M. Role of mitocondrial dynamics proteins in the pathophysiology of obesity and type 2 diabetes. *Intern J Biochem Cell Biol* 41: 1846–1854, 2009.

Address correspondence to:
Dr. Paola V. Finocchietto
Laboratory of Oxygen Metabolism
University of Buenos Aires
Córdoba 2351, 4th floor
Buenos Aires 1120
Argentina

E-mail: pfinocchietto@hotmail.com

Prof. Juan J. Poderoso
Laboratory of Oxygen Metabolism
University of Buenos Aires
Córdoba 2351, 4th floor
Buenos Aires 1120
Argentina

E-mail: jpoderos@fmed.uba.ar

Date of first submission to ARS Central, December 22, 2010; date of final revised submission, April 27, 2011; date of acceptance, April 29, 2011.

Abbreviations Used

ACC = acetyl CoA carboxylase
AICAR = AMPK inhibitor 5-amidazole-4-carboxamide-1β-D-ribofuranoside
AMPK = AMP-dependent kinase
Ara-A = AMPK inhibitor adenine 9-β-D-arabinofuranoside
ATP = adenosine triphosphate
CC = AMPK inhibitor compound C, dorsomorphin
DAF-FM = 4-amino-5-methylamino-2′,7′-difluorofluorescin diacetate
eNOS = endothelial nitric oxide synthase
H_2O_2 = hydrogen peroxide
L-Arg = L-arginine
L-NAME = L-N^Gnitroarginine methylester arginine
L-NMMA = L-N^G-monomethyl-L-arginine
MS = metabolic syndrome
mtNOS = mitochondrial nitric oxide synthase
nNOS = neuronal nitric oxide synthase
NO = nitric oxide
Ob/ob = leptin-deficient mice
ObRb = leptin receptor b
$ONOO^E$ = peroxynitrite
siRNA = small interference RNA
WAT = white adipose tissue

This article has been cited by:

1. Zoltan Giricz, Robert M. Mentzer, Roberta A. Gottlieb. 2012. Autophagy, Myocardial Protection, and the Metabolic Syndrome. *Journal of Cardiovascular Pharmacology* **60**:2, 125-132. [CrossRef]
2. Maria Carreras, Juan Jose PoderosoKinases and Mitochondrial Cycling **30**, 189-212. [CrossRef]
3. Valeria Gabriela Antico Arciuch , María Eugenia Elguero , Juan José Poderoso , María Cecilia Carreras . 2012. Mitochondrial Regulation of Cell Cycle and Proliferation. *Antioxidants & Redox Signaling* **16**:10, 1150-1180. [Abstract] [Full Text HTML] [Full Text PDF] [Full Text PDF with Links]